Influence of Added Clay Particles on the Structure and Rheology of a Hexagonal Phase Formed by an Amphiphilic Block Copolymer in Aqueous Solution

V. Castelletto, I. A. Ansari, and I. W. Hamley*

Department of Chemistry, University of Leeds, Leeds LS2 9JT, UK

Received August 28, 2002

ABSTRACT: The influence of added disklike synthetic clay particles (Laponite RDS) on the rheology and structure of the hexagonal phase formed by the poly(oxyethylene)−poly(oxypropylene)−poly(oxyethylene) triblock copolymer Pluronic P123 was investigated by dynamic shear rheometry and small-angle X-ray scattering (SAXS). The dimensions of the Laponite RDS particles were determined by analysis of the SAXS form factor, measured in dilute solution. The dynamic shear modulus of gels of P123 is found to be essentially independent of the amount of Laponite RDS up to an added Laponite solution concentration of 9 wt %, above which gelation of Laponite solutions is observed. SAXS shows that addition of Laponite particles drives a transition from a hexagonal phase of rodlike micelles at low temperature to a lamellar phase at high temperature. The transition temperature decreases as a function of the amount of added Laponite, in contrast to the width of the coexistence region between the two structures which remains nearly constant. The formation of a lamellar phase is rationalized on the basis of the entropically favored packing of the Laponite disks. The disks are found to be intercalated between the lamellae, the separation between them decreasing as Laponite concentration increases.

Introduction

Inorganic filler particles are added to soft materials such as polymers to improve their mechanical properties and also to alter properties such as color, flame resistance, or permeability. Clay particles are platelike mineral moieties based on silicates or aluminosilicates.[1] They are widely used in those applications due to their ease of availability, processability, and low cost. A recent focus has been on polymer−clay nanocomposites, in which the polymer chains are intercalated between clay layers.[2]

The interaction of inorganic particles with lyotropic mesophases is relevant to soaps and other cleaning products in which filler particles are added to surfactant solutions. From a fundamental viewpoint, it is also of interest to investigate the interplay between the self-assembly of amphiphiles and nanoparticles. A number of previous studies have considered the influence of colloidal particles[3−5] or nanoparticles[6−9] on the structure and rheology of amphiphilic lamellar phases. The incorporation of nanoparticles into the cylinders in the hexagonal phase of a surfactant solution has also been studied.[10]

In the present study, we investigate the effect of added clay particles on the structural and rheological properties of a hexagonal mesophase formed by a triblock copolymer surfactant. The clay used is the synthetic hectorite, Laponite RDS. This differs from the more widely used Laponite RD due to the presence of a peptizing agent. The triblock employed here is one of the widely used Pluronic family of poly(oxyethylene)−poly(oxypropylene)−poly(oxyethylene) (EPE) polymer surfactants—P123 ($E_{20}P_{70}E_{20}$). The sol/gel phase diagram of Laponite RD in water as a function of concentration and pH[11,12] and the aging behavior[13−15] of sols have been studied previously. We are not aware of previous studies of the structure or rheology of Laponite RDS suspensions. The phase behavior of poly(oxyethylene) homopolymer with Laponite RD has recently been investigated.[16] The influence of shear on the orientation of PEO chains and Laponite RDS particles has been studied by SANS on mixtures of these two components in aqueous solution,[17] and the rheology and flow birefringence of the same solutions have been examined.[18] The phase behavior of the block copolymer in solution has been investigated by SANS[19] and SAXS.[20]

There has been limited prior work on mixed Laponite/surfactant solutions. The adsorption of E-containing nonionic surfactants ($C_{12}E_5$ and $C_{12}E_8$, C = methyl) onto Laponite RD particles has been investigated by adsorption isotherm and small-angle neutron scattering measurements.[21] It was found that the PEO adsorbed onto the Laponite particles and that the saturation coverage in the plateau region of the adsorption isotherm corresponded to an incomplete bilayer. The area per molecule at the solid/water interface was the same as that per molecule in a lamellar bilayer. In a subsequent study, the dispersion of Laponite particles in the swollen lamellar or sponge phase of aqueous solutions of $C_{12}E_5$ and $C_{12}E_4$ was probed by SANS.[22] It was found that the solutions are stable up to a limiting concentration of surfactant (which depends on the Laponite content). Above this limiting concentration, phase separation occurred as the wavelength of the membrane undulations that stabilize the lamellar phase becomes smaller than the diameter of the Laponite disks. Because swollen phases were studied, the Laponite particles were preferentially located in the water layers, since these were thicker than the Laponite particles. In contrast, in the lamellar phase formed by the anionic surfactant AOT, the negatively charged Laponite particles formed at pH < 8 can be forced into the hydrophobic part of the surfactant bilayer when the water thickness is below that of the particles.[23]

* Author for correspondence.

10.1021/ma021396x CCC: $25.00
Published on Web 02/11/2003

Experimental Section

Materials. The synthetic clay used was Laponite RDS, obtained as a gift from Laporte Industries (now Rockwood Additives Ltd). Laponite RDS can form solutions at higher concentrations than Laponite RD, which has been used in the majority of prior studies. Solution formation is optimized by the addition of a small proportion of the peptizing agent, tetrasodium pyrophosphate (TSPP).[24] The empirical formula is then $Si_8Mg_{85.45}LI_{0.4}H_4O_{24}Na_{0.7} + Na_4P_2O_7$. When dissolved, TSPP produces pyrophosphate $(P_2O_7)^{4-}$ anions that bind to the positively charged Laponite particles. Caution is required when preparing solutions of RDS because the pyrophosphate anions are slowly hydrolyzed. The solution stability time then decreases rapidly with time.[24] This occurs more rapidly than the aging of the Laponite particles themselves (due to release of Mg^{2+} ions), which occurs on a time scale of hundreds of days.[11,15] For this reason, Laponite solutions at the highest concentration we examined (9 wt %) were prepared directly before mixing with copolymer gel for rheology or X-ray scattering experiments. Lower concentration samples were investigated within several weeks of preparation, which is within the stability window specified by the manufacturer at room temperature.[24]

For pH < 9 Laponite RD particles dissolve due to pH dissociation, whereas for pH > 10, silica dissolution occurs.[25,26] The particles are stable at pH = 9.5, so our solutions are prepared under these alkaline conditions, similar to those used in prior studies on Laponite RD.[11,12,14,26,27]

Block copolymer surfactant Pluronic P123 was obtained as a gift from Uniqema. It is a poly(oxyethylene)−poly(oxypropylene)−poly(oxyethylene) triblock copolymer, containing 30% poly(oxyethylene) and with a molecular weight of 5750 g mol^{-1}.[20] The phase diagram of P123 in water has been reported.[19]

Preparation of Mixtures. The clay dispersions were prepared by slowly adding Laponite RDS powder to ultrapure water (Milli-Q-Plus) with constant stirring for at least 15 min. The pH of the dispersions was maintained at 9.5 by adding analytical grade NaOH. The solutions, which were slightly milky white in the beginning, became transparent after 30 min of stirring. Solutions were aged for 1 week, prior to addition of block copolymer gel. Mixtures were prepared by adding aqueous gels containing Pluronic surfactant to Laponite solutions of different concentrations, such that the final mass fraction of P123 defined as $w_S = m(\text{P123})/[m(\text{P123}) + m(\text{Laponite} + \text{water})]$ was $w_S = 0.5$ (50 wt %), where m denotes mass. The mass fractions of Laponite are defined as $w_L = m(\text{Laponite})/[m(\text{Laponite}) + m(\text{water})]$, i.e., referring to the precursor solution, not accounting for the surfactant.[22] Thorough mixing was performed until the mixtures were homogeneous. The resulting dispersion was transparent and immobile and is referred to as a gel in the following, although it is emphasized that there are no cross-links between the polymer chains, and the gel formation is solely due to the packing of rodlike micelles into a hexagonal structure.

Rheology. Measurements of the dynamic shear modulus were performed using a Rheometrics RSA II controlled strain rheometer, with a shear sandwich geometry. The linear viscoelastic regime was established via strain sweeps. Subsequent isothermal frequency sweeps and isochronal (fixed frequency) temperature ramps were performed with a strain amplitude $\gamma = 0.5\%$, well within the linear regime.

SAXS. SAXS experiments were performed at the Synchrotron Radiation Source (SRS) at Daresbury Laboratory, Warrington, UK. Samples were studied either at rest or after oscillatory shear. Static experiments were performed on beamlines 8.2 and 2.1, while shear flow experiments were undertaken on beamline 16.1. All three stations are configured with an X-ray wavelength $\lambda = 1.5$ Å or $\lambda = 1.41$ Å. On station 2.1 the scattered intensity was recorded using a quadrant SAXS detector that measures intensity in the radial direction, while on both beamline 2.1 and station 16.1, the scattered intensity was recorded on a multiwire gas-filled area detector. Experiments were performed using sample−detector distance $D_{SD} =$ 8.0, 3.1, and 3.0 m for beamlines 2.1, 8.2, and 16.1, respectively. A scattering pattern from a specimen of wet collagen (rat tail tendon) was used for calibration of the q scale ($q = |\mathbf{q}| = 4\pi \sin\theta/\lambda$, where the scattering angle is 2θ) of the scattering profile.

For the static measurements the samples were mounted in sealed 1 mm thick brass cells, with an inner spacer ring to hold liquids, sealed between mica windows. The cells were connected to a water bath for temperature control.

Oscillatory shear was applied to the samples using a Rheometrics RSA II soft solids system with a shear sandwich geometry. A detailed description of the rheometer is provided elsewhere.[28,29] It enables simultaneous acquisition of SAXS and rheology data. The shear sandwich cell comprises three rectangular plates, the two external plates being fixed, while the central piece oscillates vertically. Apertures machined into the plates of the shear sandwich assembly allow transmission of the X-ray beam, being covered by Kapton polyimide windows. The sample is loaded on both sides symmetrically about the insert piece. The shear sandwich plates are perpendicular to the X-ray beam, which is incident along $\nabla\mathbf{v}$, so that the ($\mathbf{q}_v$, $\mathbf{q}_e$) plane is accessed in SAXS experiments where $\mathbf{v}$ denotes the shear direction and $\mathbf{e}$ the neutral direction.

SAXS measurements were made for temperatures ranging between 25 and 70 °C.

Results and Discussion

Optical Observations. Grillo et al. have previously investigated the insertion of Laponite particles into the lamellar phase of the two alcohol ethoxylate nonionic surfactants $C_{12}E_4$ and $C_{12}E_5$[22] that are related to the nonionic Pluronic copolymer employed here, since the hydrophilic poly(oxyethylene) block is common to both systems. They observed phase separation between a particle-rich and particle-poor phase depending on the amount of Laponite and surfactant. Inspection of our gels confirmed that all were transparent, and there was no evidence for phase separation. No attempt was made to investigate possible phase separation on varying block copolymer or Laponite concentration, since only a single concentration of P123 (50 wt %) was studied.

Rheology. The influence of Laponite particles on the mechanical properties of the Pluronic P123 block copolymer gel was examined through isochronal temperature ramps and sequences of frequency sweeps carried out at set temperature intervals. The modulus was determined from frequency sweeps for gels with Laponite concentrations from 0 to 9 wt %. It was found that at a particular temperature there was essentially no dependence on Laponite content. At a reference temperature of 25 °C and frequency $\omega = 1$ rad s^{-1}, the modulus G' was $(3.5 \pm 0.5) \times 10^3$ Pa for all samples. This result was unexpected and indicates that Laponite cannot be used as an additive to improve the elasticity of these block copolymer gels. The observation may be rationalized by the insertion of Laponite particles into the block copolymer microstructure, as discussed below. Temperature ramps at constant frequency indicated a decrease in modulus on increasing temperature.

Frequency sweeps were also performed for gels containing 0−9 wt % Laponite. Figure 1 shows data for a 3 wt % gel. Although not strictly valid for microstructured fluids, but commonly used nonetheless, time−temperature superposition was performed (reference temperature = 55 °C) to facilitate comparison of the frequency response at different temperatures. At low frequencies, the scalings $G' \sim \omega^{0.45}$ and $G'' \sim \omega^{0.1}$ are found for the two higher temperatures. Both are characteristic of microstructured fluids, in particular lamellar or hexagonal phases formed by block copolymers or

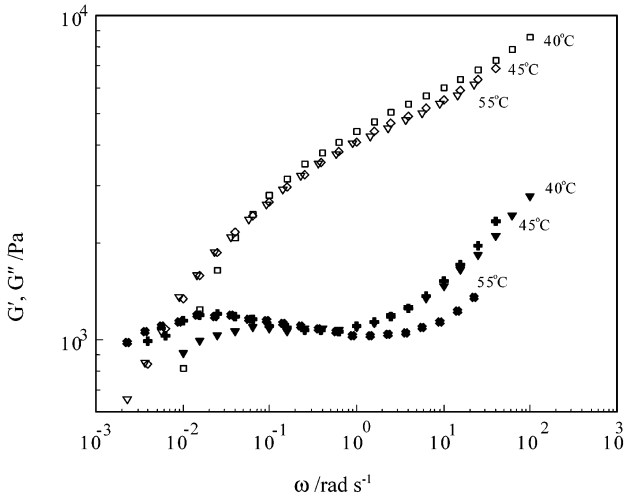

Figure 1. Time−temperature superposed (reference temperature = 55 °C) frequency sweep data for three temperatures (indicated) for the gel containing 3 wt % RDS; G' (open symbols) and G'' (closed symbols).

surfactants.[30] A steeper frequency dependence for both moduli is apparent at $T = 40$ °C, which is in the single-phase hexagonal region, whereas $T = 45$ and 55 °C are in the two-phase hexagonal (H) + lamellar (L) phase coexistence region (Figure 5a). Thus, there is some evidence for changes in the dynamic mechanical response as a function of temperature at very low frequency.

SAXS. Laponite particles have previously been shown to be platelike. Analysis of the form factor from SAXS experiments on dilute suspensions of Laponite RD indicates a plate diameter $2R = 25-30$ nm and a thickness $H = 1$ nm.[11,15] As mentioned above, we have used Laponite RDS, which differs from Laponite RD due to the presence of bound pyrophosphate anions. The effective dimensions of the particles might therefore be influenced, and so SAXS measurements were performed to determine the plate dimensions. The SAXS intensity of diluted solutions of cylindrical particles with thickness H and radius R is given by[31]

$$I(q) = n_p \int_0^{\pi/2} \left[\frac{\sin(qH\cos\alpha)}{(qH\cos\alpha)} \frac{2J_1(qR\sin\alpha)}{(qR\sin\alpha)} \right]^2 \sin\alpha \, d\alpha \quad (1)$$

where n_p is a normalization constant proportional to the number density of particles, J_1 is the Bessel function of first order, and α is the angle between the main axis of the cylinder and the scattering vector q. The SAXS data for 2 wt % Laponite RDS in aqueous solution at pH = 10 are shown in Figure 2, together with the SAXS intensity calculated from eq 1 from which we estimated $2R = 35.3 \pm 0.3$ nm and $H = 2.1 \pm 0.1$ nm. The deviations at small q are due to interparticle interference effects.[15,31] Compared to the previous results for Laponite RD,[11,15] the diameter and thickness are both increased due presumably to the adsorbed anions.

The structure of gels containing 0−9 wt % added Laponite RDS at pH = 10 was determined by SAXS in the temperature range from 25 to 75 °C. The main feature of the SAXS patterns for gels of P123 in the absence of Laponite is a series of Bragg reflections. Figure 3 shows a representative SAXS profile, with five reflections, obtained at 46 °C. The peaks are located in

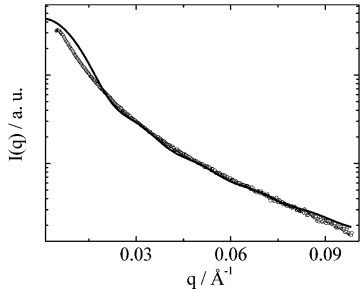

Figure 2. SAXS profile measured for a 2 wt % Laponite RDS aqueous solution (○) and the calculated form factor for an isolated disk-shaped particle (—) using eq 1. In the model, the particle diameter and thickness are $2R = 35.3$ nm and $H = 2.1$ nm, respectively.

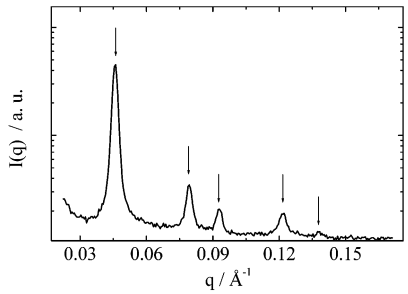

Figure 3. SAXS profile for 50 wt % P123 at 46 °C. The arrows indicate the position of the measured reflections.

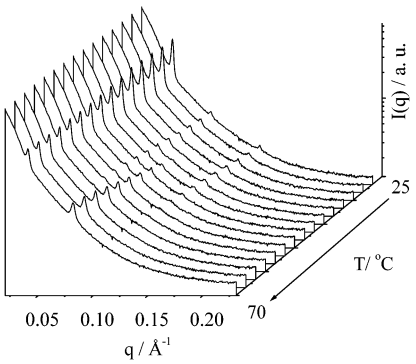

Figure 4. Temperature dependence of the SAXS intensity profile measured for a P123 gel containing 7 wt % Laponite.

the positional ratio $1:(3)^{1/2}:(4)^{1/2}:(7)^{1/2}:(9)^{1/2}$, as expected for a H lattice. These results are consistent with the previously reported phase diagram of the P123 in water.[19]

Figure 4 shows the temperature dependence of the SAXS profile measured for a P123 gel containing 7 wt % Laponite RDS. A discontinuity in the position of a higher-order reflection and in the intensity of the first-order reflection is apparent at $T = 53$ °C. The SAXS intensity as a function of the temperature was also recorded for P123 gels with 3−7 wt % Laponite RDS. We measured the position of the scattering peaks from each SAXS profile, and the results are contained in Figure 5, which shows the position of the scattering peaks as a function of temperature.

Figure 5 shows that at low temperature the gels are characterized by three to five reflections with a positional ratio $1:(3)^{1/2}:(4)^{1/2}:(7)^{1/2}:(9)^{1/2}$ corresponding to the reflections from a H structure.[32] In contrast, at high temperature only two or three reflections were measured with a positional ratio 1:2:3 within the experimental error, which are indexed to the 100, 200, and 300 reflections, respectively, of a L phase.[32] We present

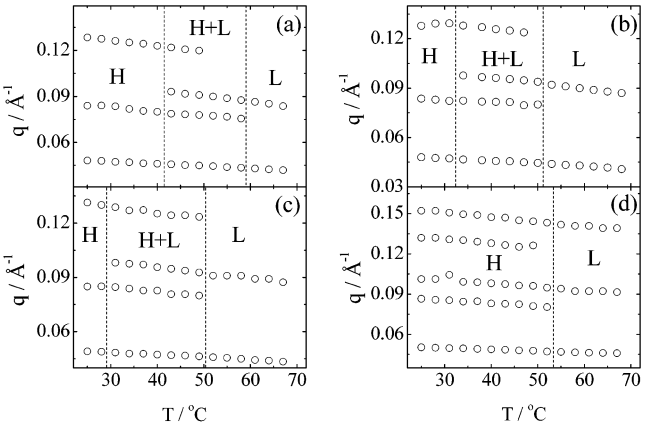

Figure 5. Temperature dependence of the Bragg peak positions for 50 wt % P123 with (a) 3, (b) 4.5, (c) 7, and (d) 9 wt % Laponite RDS. The traced lines divide the regions of hexagonal (H), lamellar (L), and H/L phase coexistence. The standard deviations of the Bragg peak positions, have been omitted because the error bars are smaller than the symbols used to plot the data.

shortly data from shear-oriented specimens that indicate that indeed there is a structural phase transition rather than just a change in orientation (causing the loss of certain reflections). For intermediate temperatures, and for samples containing between 3 and 7 wt % added Laponite, a set of reflections in the positional ratio $1:(3)^{1/2}:(4)^{1/2}:(7)^{1/2}$ are present, suggesting that both H and L orders coexist in the system (Figure 5). A transition from H to L structures is not observed for a 50 wt % gel of the copolymer alone between 25 and 75 °C.[19] Therefore, the results shown in Figure 5 suggest that the addition of Laponite RDS to the system induces an H to L phase transition at high temperature. The transition moves to lower temperatures with increasing Laponite concentration, except for the highest concentration Laponite gel.

To confirm a structural transition, SAXS patterns were obtained from samples aligned using large-amplitude oscillatory shear (frequency $\omega = 100$ rad s^{-1} and strain amplitude $A = 70\%$). Figure 6 shows the two-dimensional SAXS patterns obtained at rest following shear, for a gel with 9 wt % Laponite RDS, at 30 °C (Figure 6a) and 60 °C (Figure 6b). In both cases, two pairs of equatorial reflections are observed. At 30 °C these are in the positional ratio $1:(3)^{1/2}$, and at 60 °C they are in the ratio 1:2 . The former is consistent with a shear-aligned H phase in which the cylinder axis is parallel to the direction of flow, while the latter results indicate that oscillatory shear orients the layers in the L phase perpendicular to the ($\mathbf{q}_v$, $\mathbf{q}_e$) plane, with the lamellar normal parallel to the neutral axis (Figure 7). The presence of the peaks with positions in the ratio $1:(3)^{1/2}$ in the H phase indicates that the sample is not a single crystal,[33,34] since in a single crystal only one or other of these reflections would be accessed, depending on the orientation of the hexagonal lattice with respect to the shear plane. Either the sample is a two-dimensional powder in which the hexagonal lattice is rotated around the cylinder axis or the two orientations of the hexagonal lattice rotated 30° with respect to one another coexist, as illustrated in Figure 7a.

From the location of the SAXS peaks it is possible to determine the domain spacing in the H and L phases as a function of temperature. In particular, the average distance between cylinders in the H phase, $d = 2\pi/q_0$

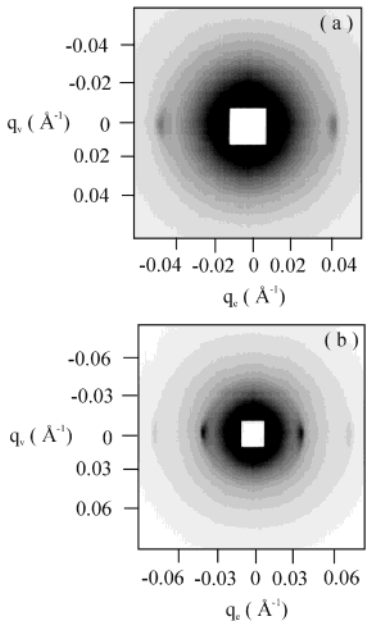

Figure 6. SAXS pattern in the ($\mathbf{q}_v$, $\mathbf{q}_e$) plane obtained at (a) 30 °C (the second-order peak is not shown in the figure because the contrast scale used does not allow first and second-order reflections to be shown simultaneously) and (b) 60 °C for a gel containing 9 wt % added Laponite RDS, at rest after oscillatory shear in the shear sandwich at a frequency $\omega = 100$ s^{-1} and strain amplitude $A = 70\%$.

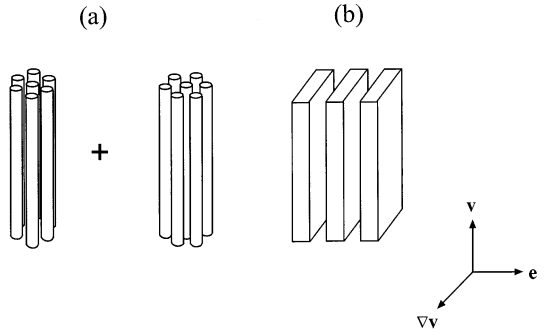

Figure 7. (a) Coexisting orientations of hexagonal lattice with respect to the (**v**,**e**) plane that must be present in order to observe reflections in the positional ratio $1:\sqrt{3}$. (b) Orientation of the lamellae obtained via an epitaxial transition from the aligned H phase in (b).

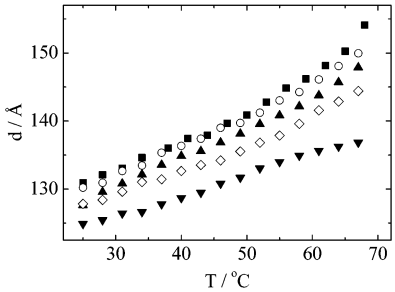

Figure 8. Temperature dependence of the mean distance between objects $d = 2\pi/q_0$ for gels containing (▲) 0, (○) 3, (◇) 4.5, (■) 7, and (▼) 9 wt % added Laponite RDS.

(q_0 = position of the first scattering peak), is calculated in the same way as the interlayer distance d in the L phase. Figure 8 shows that the domain spacing increases with temperature, and there are no discontinuities across the phase transition boundary. Furthermore, the domain spacing does not change appreciably upon addition of up to 7 wt % Laponite (indeed, Figure

8 shows that it oscillates around the value for 0 wt % Laponite) but decreases for a gel containing 9 wt % Laponite RDS. The continuous increase of the distance between the cylindrical micelles in the pure P123 gel in Figure 8 may be due to the increase in aggregation number observed for P123 on increasing temperature,[19] which in turn results from the poorer solvent quality for E chains.

It should be noted that a linear decrease in d with the increase of Laponite content in the sample is expected for samples in the L phase (Figures 5 and 8). In a L phase consisting of bilayer sheets of constant thickness, the domain spacing is given by[35]

$$d = \delta/\phi \tag{2}$$

where ϕ is the volume fraction of solute in the system and δ is the hydrophobic layer thickness. In our work ϕ increases upon addition of Laponite to the P123/water system, but it does not lead to a continuous decrease of d (Figure 8). Therefore, our results suggest that for the P123/water system the addition of Laponite also modifies the hydrophobic layer thickness.

The domain spacing in the H phase plotted in Figure 8 can be compared to the previously published value. Holmqvist et al.[20] measured $d = 120.4$ Å for a 45 wt % P123 gel at $T = 25$ °C, which is in good agreement with the values in Figure 8.

The fact that q_0 changes continuously across the transition (Figures 5 and 8) indicates that the transition between H and L structures is epitaxial. Epitaxial transitions between hexagonal and lamellar phases have previously been reported for lyotropic liquid crystals[36,37] and block copolymer melts[38,39] (in which case the lamellae may be metastable perforated lamellae); however, the transition in these cases occurs via an intermediate bicontinuous cubic phase. There is no evidence for a bicontinuous cubic structure in our SAXS data, which is consistent with a direct transition. To our knowledge, such a transition has not been reported before. We propose that the formation of a bicontinuous cubic structure with an interconnected near-constant mean curvature surface is inhibited by the presence of the Laponite disks.

It is possible to undertake a qualitative analysis of the order of the anisotropic particles dispersed in the L phase. Two relevant distances can be distinguished: the center-to-center particle separation, D_{2D}, and the intermembrane separation distance, D. The two-dimensional particle−particle separation D_{2D}, for particles located on average in the mid-plane between the surfactant lamellae separated by a water thickness D, is given by[22]

$$D_{2D} = \sqrt{\frac{2V_L(C_L + \rho_L)}{3DC_L}} \tag{3}$$

where V_L is the volume of a Laponite disk, C_L is the mass of dried Laponite divided by the mass of water, and $\rho_L = 2.53$ is the density of Laponite with respect to water. Using the parameters from the form factor fit to the SAXS profile from a Laponite disk (Figure 2), $V_L = \pi R^2 H = 1923.3$ nm^3. In eq 3, the intermembrane separation distance $D = d - \delta$ is expressed as a function of the hydrophobic layer thickness, where the d values are taken from Figure 8, and δ is given by eq 2. The volume fraction of polymer in the P123/Laponite/water system is

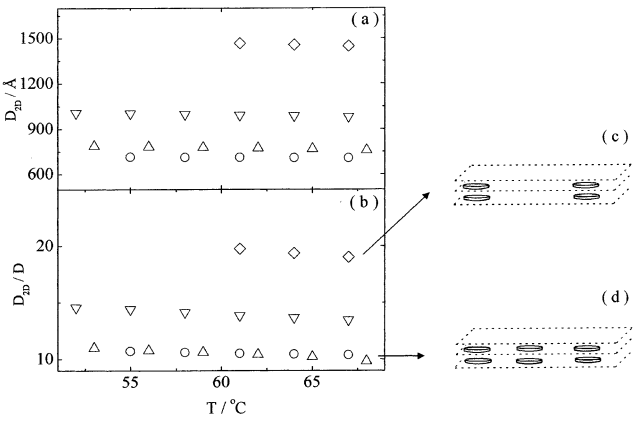

Figure 9. Dependence of (a) D_{2D} and (b) D_{2D}/D on temperature for a 50 wt % P123 gel with (◇) 3, (▽) 4.5, (△) 7, and (○) 9 wt % added Laponite RDS. Shown alongside are sketches indicating the size and spacing of disks compared to the lamellar spacing for (c) 3 wt % added Laponite at 75 °C and (d) 9 wt % added Laponite at 67 °C.

$$\phi = \frac{w_S\rho_L(1 + C_L)}{d_S\rho_L + \rho_L w_S(1 - d_S) + C_L(\rho_S + w_S(\rho_L - \rho_S))} \tag{4}$$

where w_S is the mass fraction of surfactant in the sample ($w_S = 0.5$). The parameter $\rho_S = 1.05$ is the density of P123 relative to water.[20]

Figure 9 shows the evolution of D_{2D} and the fraction D_{2D}/D as a function of temperature, for different concentrations of Laponite RDS, within the L phase. As expected, the average distance between the clay disks decreases with increasing Laponite concentration (Figure 9a) as does the ratio D_{2D}/D (Figure 9b). Temperature seems to have little effect on this behavior. Figure 9b−d shows that the center-to-center distance is always higher than the intermembrane distance, ensuring enough space for the disks to freely spread between the lamellae.

These calculations on the separation of Laponite particles within and between layers confirm that there is ample space for them to be intercalated between lamellae. It is thus proposed that the hexagonal-to-lamellar transition is driven by the increase in packing entropy of the disks in the lamellar phase, compared to the hexagonal phase. Assuming that the particles are preferentially located in the aqueous region, the volume available to the particles is smaller in the hexagonal phase since the packing fraction of surfactant is higher. The concentration dependence of the transition arises because the excluded volume available to the particles (more of which is "explored" by the Brownian motion of particles at high temperature) decreases with increasing particle concentration.

To obtain an insight into the effect of the Laponite on the elasticity of the layers in the lamellar phase, we used the model of Caillé[40] to fit the shape of the SAXS reflections. For one-dimensional systems the scattered intensity should exhibit an asymptotic power-law behavior $S(q) \sim |q - q_{0,m}|^{-2+\eta_m}$, where η_m is the mth-order Caillé parameter and $q_{0,m}$ is the position of the mth-order scattering peak.[40,41] This model differs from the lamellar phase structure factor[42] previously used by Grillo et al.[22] because the later does not describe the intensity satisfactorily away from the peaks. Therefore,

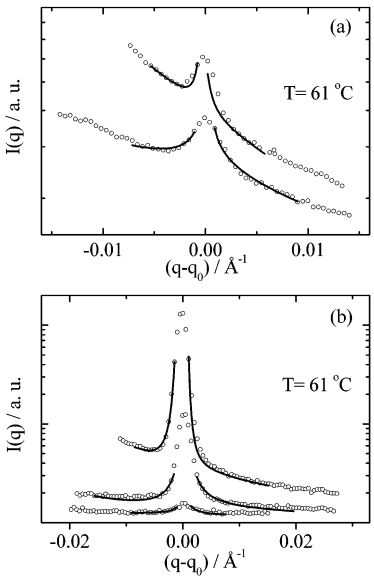

Figure 10. (○) Scattering peaks in the SAXS curves, on a shifted scale, plotted for a 50 wt % P123 sample with (a) 7 wt % Laponite; top: $m = 1$, bottom: $m = 2$, and (b) 9 wt % Laponite, top to bottom $m = 1, 2, 3$. The solid lines represent fits using the Caillé structure factor (see text).

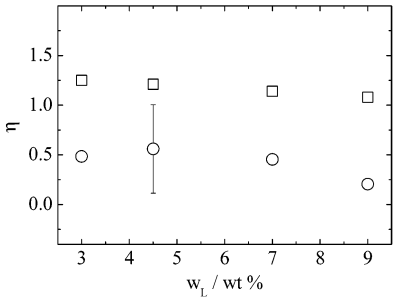

Figure 11. Dependence of the Caillé parameter on concentration of added Laponite: (○) Caillé parameter extracted from fitting peaks in the SAXS profiles (Figure 10), (□) calculated according to the Helfrich model. The standard deviation of the fitted Caillé parameter is shown for 4.5 wt % added Laponite.

only the scattering data near the peaks were fitted. Representative results obtained from fitting the asymptotic behavior of the scattering peaks in the lamellar phase for 7 and 9 wt % added Laponite at 61 °C are shown in Figure 10a,b. To make the fitting, an empirically determined background $\sim(C_1/q^{2.5}) + C_2$ (where C_1 and C_2 are constants) was subtracted from the scattering curves.

An averaged value of the Caillé parameter, $\bar{\eta}$, was obtained using the set of η_m values for a particular SAXS profile, i.e., calculating the average of $\eta = \eta_m/m^2 = (q_0^2 k_B T)/[8\pi(KB)^{1/2}]$. Here K and B are elastic and compression moduli for lamellae, respectively.[40,41] The dependence of $\bar{\eta}$ on concentration of added Laponite (at a constant temperature $T = 61$ °C) is illustrated in Figure 10, together with the Caillé parameter calculated on the basis of the theory of Helfrich developed for the lamellar phase of nonionic surfactants.[43] In this model $\eta = {}^4/_3(1 - \delta/d)^2$.[41] Figure 11 shows that the experimental $\bar{\eta}$ is lower than predicted by the Helfrich model, indicating "harder" lamellar lamellae than expected purely on the basis of entropic interactions between fluctuating lamellae. This suggests some interaction between the Laponite and (presumably) the poly(oxyethylene) chains extending into the water layer. This contrasts with the results of Grillo et al.[22] on low molar mass nonionic surfactants, possibly because in their case the E chains are extremely short and do not adsorb onto the particles. It is also evident that both $\bar{\eta}$ and the Caillé parameter predicted by the Helfrich model are essentially independent of Laponite content in the sample. This indicates that the product KB is not influenced by added Laponite. This could be due to either constant values of K and B or a compensation between an increase in one and a decrease in the other. Unfortunately, at present we are unable to determine the two quantities separately, although methods exist to extract K from the concentration dependence of the domain spacing.[44] Grillo et al. also found η to be independent of the amount of Laponite RD added to the lamellar phase of nonionic surfactant $C_{12}E_4$.[22]

Summary

A transition between a hexagonal phase formed from rodlike micelles and a lamellar phase has been observed in a mixture of a concentrated block copolymer in water upon addition of synthetic clay, Laponite RDS, up to a concentration close to the gel point of alkaline solutions of Laponite. The block copolymer studied was a poly(oxyethylene)−poly(oxypropylene)−poly(oxyethylene) triblock, Pluronic P123, which is a nonionic surfactant. This work complements prior work on the influence of added Laponite on the lamellar and sponge phases of low molar mass nonionic surfactants.[22] The addition of Laponite has essentially no influence on the magnitude of the dynamic shear moduli. In frequency sweeps, subtle changes in the low-frequency response occur across the transition region between hexagonal and lamellar phases.

The transition from hexagonal phase in a 50 wt % block copolymer solution to a lamellar phase on addition of Laponite, at sufficiently high temperature, is tentatively ascribed to a difference in packing entropy of the disklike particles in the two phases. There is a "packing frustration" for disks in the hexagonal phase due to a reduced excluded volume. The transition temperature decrease with increasing Laponite concentration, and there is a wide biphasic region, except for the highest Laponite concentration (9 wt %). The domain spacings in the hexagonal and lamellar phases were determined from the position of the peaks in the SAXS pattern and were found to increase with temperature, although no systematic dependence on Laponite concentration was observed.

The form factor of the Laponite particles confirmed them to be disklike, with a diameter $2R = 35$ nm and thickness $H = 2$ nm. Using these dimensions, together with the density and amount of added Laponite and the calculated thickness of the water layer between block copolymer lamellae, enabled the average separation between Laponite particles to be calculated in the lamellar phase. It was thus shown that there was ample space to accommodate them within the water layer. The spacing between particles decreased with increasing Laponite content, as expected.

The structure factor in the vicinity of the Bragg peaks in the lamellar phase was analyzed using the Caillé model, from which an average Caillé exponent was determined from fits to all orders of reflection. This was found to be essentially independent of Laponite content, showing that the "stiffness" of the lamellae, quantified as $(KB)^{1/2}$, where K and B are elastic and compression

moduli, respectively, does not depend on the amount of added Laponite.

References and Notes

(1) Hamley, I. W. *Introduction to Soft Matter*; John Wiley: Chichester, 2000.
(2) Giannelis, E. P.; Krishnamoorti, R.; Manias, E. *Adv. Polym. Sci.* **1999**, *138*, 108−147.
(3) Salamat, G.; Kaler, E. W. *Langmuir* **1999**, *15*, 5414−5421.
(4) Arrault, J.; Poon, W. C. K.; Cates, M. E. *Phys. Rev. E* **1999**, *59*, 3242−3252.
(5) Basappa, G.; Suneel; Kumaran, V.; Nott, P. R.; Ramaswamy, S.; Naik, V. M.; Rout, D. *Eur. Phys. J. B* **1999**, *12*, 269−276.
(6) Ramos, L.; Fabre, P.; Dubois, E. *J. Phys. Chem.* **1996**, *100*, 4533−4537.
(7) Ponsinet, V.; Fabre, P. *J. Phys. Chem.* **1996**, *100*, 5035−5038.
(8) Hamdoun, B.; Ausserre, D.; Cabuil, V.; Joly, S. *J. Phys. II* **1996**, *6*, 503−510.
(9) Ponsinet, V.; Fabre, P. *J. Phys. II* **1996**, *6*, 955−960.
(10) Ramos, L.; Fabre, P.; Ober, R. *Eur. Phys. J. B* **1998**, *1*, 319−326.
(11) Mourchid, A.; Delville, A.; Lambard, J.; Lécolier, E.; Levitz, P. *Langmuir* **1995**, *11*, 1942−1950.
(12) Mourchid, A.; Lécolier, E.; Van Damme, H.; Levitz, P. *Langmuir* **1998**, *14*, 4718−4723.
(13) Mourchid, A.; Levitz, P. *Phys. Rev. E* **1998**, *57*.
(14) Knaebel, A.; Bellour, M.; Munch, J.-P.; Viasnoff, V.; Lequeux, F.; Harden, J. L. *Europhys. Lett.* **2000**, *52*, 73−79.
(15) Kroon, M.; Wegdam, G. H.; Sprik, R. *Phys. Rev. E* **1996**, *54*, 6541−6550.
(16) Zebrowski, J.; Prasad, V.; Zhang, W.; Walker, L. M.; Weitz, D. A. Preprint, 2002.
(17) Schmidt, G.; Nakatani, A. I.; Butler, P. D.; Han, C. C. *Macromolecules* **2002**, *35*, 4725−4732.
(18) Schmidt, G.; Nakatani, A. I.; Han, C. C. *Rheol. Acta* **2002**, *41*, 45−54.
(19) Wanka, G.; Hoffmann, H.; Ulbricht, W. *Macromolecules* **1994**, *27*, 4145−4159.
(20) Holmqvist, P.; Alexandridis, P.; Lindman, B. *J. Phys. Chem. B* **1998**, *102*, 1149−1158.
(21) Grillo, I.; Levitz, P.; Zemb, T. *Eur. Phys. J. B* **1999**, *10*, 29−34.
(22) Grillo, I.; Levitz, P.; Zemb, T. *Eur. Phys. J. E* **2001**, *5*, 377−386.
(23) Grillo, I.; Levitz, P.; Zemb, T. *Langmuir* **2000**, *16*, 4830−4839.
(24) http://www.laponite.com.
(25) Thompson, D. W.; Butterworth: J. T. *J. Colloid Interface Sci.* **1992**, *151*, 236−243.
(26) Cousin, F.; Cabuil, V.; Levitz, P. *Langmuir* **2002**, *18*, 1466−1473.
(27) Levitz, P.; Lecolier, E.; Mourchid, A.; Delville, A.; Lyonnard, S. *Europhys. Lett.* **2000**, *49*, 672−677.
(28) Pople, J. A.; Hamley, I. W.; Fairclough, J. P. A.; Ryan, A. J.; Komanschek, B. U.; Gleeson, A. J.; Yu, G.-E.; Booth, C. *Macromolecules* **1997**, *30*, 5721−5728.
(29) Hamley, I. W.; Pople, J. A.; Gleeson, A. J.; Komanschek, B. U.; Towns-Andrews, E. *J. Appl. Crystallogr.* **1998**, *31*, 881−889.
(30) Larson, R. G. *The Structure and Rheology of Complex Fluids*; Oxford University Press: New York, 1999.
(31) Guinier, A.; Fournet, G. *Small Angle Scattering of X-rays*; Wiley: New York, 1955.
(32) *International Tables for X-ray Crystallography*; Kynoch Press: Birmingham, 1959; Vol. II.
(33) Koppi, K. A.; Tirrell, M.; Bates, F. S.; Almdal, K.; Mortensen, K. *J. Rheol.* **1994**, *38*, 999−1027.
(34) Fairclough, J. P. A.; Salou, C. L. O.; Ryan, A. J.; Hamley, I. W.; Daniel, C.; Helsby, W. I.; Hall, C.; Lewis, R. A.; Gleeson, A. J.; Diakun, G. P.; Mant, G. R. *Polymer* **2000**, *41*, 2577−2582.
(35) Luzzati, V. *Biological Membranes*; Academic Press: London, 1968.
(36) Rançon, Y.; Charvolin, J. *J. Phys. Chem.* **1988**, *92*, 2646−2651.
(37) Clerc, M.; Levelut, A. M.; Sadoc, J. F. *J. Phys. II* **1991**, *1*, 1263−1276.
(38) Zhao, J.; Majumdar, B.; Schulz, M. F.; Bates, F. S.; Almdal, K.; Mortensen, K.; Hajduk, D. A.; Gruner, S. M. *Macromolecules* **1996**, *29*, 1204−1215.
(39) Vigild, M. E.; Almdal, K.; Mortensen, K.; Hamley, I. W.; Fairclough, J. P. A.; Ryan, A. J. *Macromolecules* **1998**, *31*, 5702−5716.
(40) Caillé, M. A. *C. R. Acad. Sci. Paris* **1972**, *274*, 891−893.
(41) Safinya, C. R.; Roux, D.; Smith, G. S.; Sinha, S. K.; Dimon, P.; Clark, N. A.; Bellocq, A. M. *Phys. Rev. Lett.* **1986**, *57*, 2718−2721.
(42) Nallet, F.; Laversanne, R.; Roux, D. *J. Phys. II* **1993**, *3*, 487−502.
(43) Helfrich, W. *Z. Naturforsch., A: Phys. Sci.* **1978**, *33*, 305−315.
(44) Roux, D.; Nallet, F.; Freyssingeas, E.; Porte, G.; Bassereau, P.; Skouri, M.; Marignan, J. *Europhys. Lett.* **1992**, *17*, 575−581.

MA021396X